Review of the Nanostructuring and Doping Strategies for High-Performance ZnO Thermoelectric Materials

Suraya Sulaiman [1,2,*], **Izman Sudin** [1], **Uday M. Basheer Al-Naib** [1,3] and **Muhammad Firdaus Omar** [4]

1 School of Mechanical Engineering, Faculty of Engineering, Universiti Teknologi Malaysia, Skudai 81310, Johor, Malaysia; izman@utm.my (I.S.); uday@utm.my (U.M.B.A.-N.)
2 Faculty of Manufacturing and Mechatronic Engineering Technology, Universiti Malaysia Pahang, Pekan 26600, Pahang, Malaysia
3 Centre for Advanced Composite Materials (CACM), Institute for Vehicle Systems and Engineering, Universiti Teknologi Malaysia, Skudai 81310, Johor, Malaysia
4 Physics Department, Faculty of Science, Universiti Teknologi Malaysia, Skudai 81310, Johor, Malaysia; firdausomar@utm.my
* Correspondence: surayas@ump.edu.my

Abstract: Unique properties of thermoelectric materials enable the conversion of waste heat to electrical energies. Among the reported materials, Zinc oxide (ZnO) gained attention due to its superior thermoelectric performance. In this review, we attempt to oversee the approaches to improve the thermoelectric properties of ZnO, where nanostructuring and doping methods will be assessed. The outcomes of the reviewed studies are analysed and benchmarked to obtain a preliminary understanding of the parameters involved in improving the thermoelectric properties of ZnO.

Keywords: thermoelectric material; nanostructure approach; doping approach; nanoparticle; zinc oxides

1. Introduction

Pioneering studies on thermoelectric materials began in 1822. Thermoelectric was first proposed in the 1820s to convert waste energies from automobiles and manufacturing to useful electrical energies [1–4], which can potentially bring lucrative economic profits [1,5,6]. Thermoelectric materials can be applied in woodstove and diesel power plants for optimal power efficiency [5]. The ideal heat-to-electricity conversion rate in a typical thermoelectric device ranges from 15% to 20% [7]. These rates can significantly reduce the usage of non-renewable energy sources [8]. Despite the promising potential of thermoelectric conversion, the current energy conversion rate is only around 7% to 10% [1,9] due to the unsatisfactory performances of the existing thermoelectric materials, which do not meet the commercial requirement. Thus, studies have focused on synthesising high-quality and excellent-performance thermoelectric materials.

In the 1950s, researchers focused on conventional materials such as Bismuth telluride (Bi_2Te_3,) lead telluride (PbTe) and Silicon Germanium (Si-Ge) [10,11], which contain heavy elements and covalent bonding characteristics, aiming to reduce the thermal conductivity and increase the electron mobility, respectively [12,13]. The main figure of merit (ZT) of these materials ranged between one and two [13–15], which are sufficient for practical applications in thermoelectric fields [5]. However, the poor durability and chemical stability at high temperatures of these materials limit their feasibilities in thermoelectric applications. At the same time, these materials have high synthesis complexity and are toxic, further limiting their feasibilities in practical thermoelectric applications [5,12–14,16]. Thus, in the mid-1990s, the investigation paradigm switched from optimising conventional thermoelectric materials to exploratory ventures of novel thermoelectric materials. Of the investigated

materials, metal oxides offered excellent stability and oxidation resistance and are primarily safe [12–14,17]. These properties complement the limitations of the conventional thermoelectric materials (Bi_2Te_3, PbTe, and Si-Ge), which were widely studied in the 1950s. Unfortunately, the major drawback of metal oxides is the lower ZT values. The low carrier mobility and high thermal conductivity in metal oxides [12,14] result in smaller ZT values than that of the conventional non-oxides materials. However, one characteristic of the metal oxides is opposite to that of conventional thermoelectric materials, whereby the ZT value of metal oxide can be significantly increased at higher temperatures. Therefore, suggesting various possibilities of elevated temperature operations in metal oxides [12]. Having said that, many studies have been reported on the excellent thermoelectric properties of metal oxides. For instance, zinc oxide (ZnO) exhibited a high ZT value of 0.44 at 1000 K [16] and a ZT value of 0.52 at 1100 K [18]. In order to achieve this ZT value, a nanostructured approach and chemical doping strategy were employed.

The ZT value of thermoelectric materials is determined using an equation ZT = $(S^2\sigma T)\kappa^{-1}$, where S is the Seebeck coefficient, σ is the electrical conductivity, κ is thermal conductivity, and T is temperature [15,19]. According to the literature, the ZT value should be at least 1 to 1.25 for thermoelectric usage [15]. From the equation, the term $S^2\sigma$ is also known as the power factor (PF) [2,20–28]. Larger the ZT value leads to a higher heat-to-energy conversion rate, where the materials exhibit better thermoelectric performances. To achieve that, the PF should be maximised, and the thermal conductivity value should be kept to the lowest possible [29]. However, various parameters are involved in optimising the PF [30]. The parameters include the Seebeck coefficient and thermal conductivity, which are theoretically interdependent [13,24,29,30]. The alteration of these parameters involves complex, fundamental physics, including modification of carrier concentration, band structures, vacancies, defects, etc. [29]. These complex insights significantly disrupted the development of ZnO thermoelectric materials [5,31,32].

2. Zinc Oxide (ZnO)

ZnO is a promising n-type thermoelectric material [2,33–37] and an iconic representation of group II-IV compound semiconductor material [6,15,23,38,39]. The n-type semiconductor behaviour originated from the ionisation of excess zinc atoms in interstitial positions and the presence of oxygen vacancies [36]. ZnO is naturally found in the mineral called zincite [35], appears as a white powder and is soluble in water and alcohol. Due to its chemical structure, it has excellent physical and chemical properties, high electron mobility and can be easily synthesised [20,33,34,39–41]. Moreover, due to its abundance, ZnO can be obtained at a low cost [2,35,37]. It is also safer and of low toxicity [1,2,34,37,42], compared to other telluride-based nanomaterials such as PbTe and tin telluride (SnTe) [3,25,33,35,43,44].

ZnO crystallises in hexagonal wurtzite (Wz) structure with two lattice parameters, a and c (a = 3.249 and c = 5.206 Å) and space group P63mc (186) [6,15,20,23,38,45,46]. Each anion is surrounded by four cations at the corners of a tetrahedron and vice versa [45,47,48] (Figure 1a). Wz structure contributes to the high stability of ZnO [39], whereby it can also act as a benchmarking index in determining the doping effects in ZnO [20]. As indicated in Figure 1b, the X-Ray diffraction of ZnO exhibited unique and iconic peaks for ZnO crystals [47,49]. Apart from that, ZnO has a wide and direct bandgap semiconductor with 3.3 eV at room temperature [38,46] and ~3.3–3.37 eV at 300 K [23,44,50,51] with a large exciton binding energy of 60 meV at room temperature [15,22,35,42,44]. The bandgap reduces electronic noise and demonstrates superior electrical durability [40]. Moreover, the chemical and mechanical stability make ZnO an ideal candidate for high-temperature, high voltage thermoelectric applications [22,38,43,44,52].
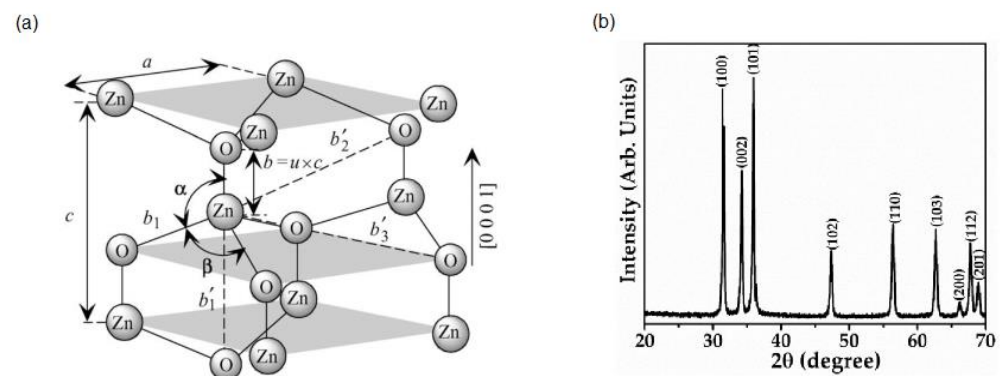
Figure 1. (**a**) A schematic of the hexagonal Wz ZnO crystal structure with lattice parameters a and c, bond length u, the nearest neighbour distance b, and three types of second-nearest-neighbour distances b´$_1$, b´$_2$, and b´$_3$. [48], (**b**) A powder diffraction pattern for ZnO [49].

Despite the promising potential of ZnO thermoelectric materials, the drawbacks in realising ZnO-based thermoelectric materials include poor electrical conductivity and high thermal conductivity. The thermal conductivity of ZnO is about 49 W/mK at 300 K and 10 W/mK at 1000 K, attributed to the stable covalent bond [16]. This disadvantage limits the ZT value of ZnO, which affects its feasibility in thermoelectric applications. Therefore, to enhance the thermoelectric properties of ZnO, various approaches, including foreign-particle doping and nanostructuring, are performed.

3. Enhancing the Thermoelectric Performance of ZnO

ZnO has a high Seebeck coefficient [34] between −350 and −430 µV/K [40,53]. These drawbacks lead to a poor ZT value of less than 0.01, which is undesirable for thermoelectric applications [14–16,54]. Many strategies have been attempted to obtain higher ZT values and lower thermal conductivity in ZnO ceramics. The strategies used include nanostructuring approach [2,50] focusing on the reduction of thermal conductivity [2,50,51,55], doping [2,21,50,51,55–57] and nanostructuring [58–61]. The following sections discuss the common approaches to enhancing the PF and lowering the thermal conductivity of ZnO, which include nanostructuring and doping approaches. This review seeks to provide a comprehensive compilation of the available strategies for enhancing the thermoelectric properties of ZnO, which can serve as a useful preliminary guide for the further development of ZnO in thermoelectric applications.

3.1. Nanostructure Approach

To date, substantial research activities have been conducted on nanostructuring thermoelectric materials. The nanostructuring approach has been reported to effectively reduce the thermal conductivity of many thermoelectric material systems to improve their thermoelectric properties. Fundamentally, the nanostructuring approach is the growth of superfine nanostructured materials [36,62]. The size of nanostructures/nanoparticles ranges between 1 and 100 nm, while non-nanostructured materials fall between 100 and 1000 nm, commonly referred to as submicron [63,64]. The altering of the synthesis method produces ZnO materials with improved thermoelectric properties.

Figure 2 indicates the effects of the nanostructuring and non-nanostructuring approaches on ZT values of ZnO ceramics over temperature. The dashed lines in Figure 2 [1,2,16,18,50,65] represent the nanostructuring approach and the solid lines represent the non-nanostructuring approach [21–23,34,51,53,55,66,67]. In the nanostructuring approach, strong phonon scattering is applied at grain boundaries, and the grain sizes are refined to lower the thermal conductivity. The correlation between ZnO grain size and its

corresponding thermal conductivity can be explained using the Callaway model [15,68,69], where the thermal conductivity of nanostructured ZnO can be expressed as:

$$\kappa = CT^3 \int_0^{\theta_D/T} \frac{x^4 e^x (e^x - 1)^{-2}}{\alpha T^4 x^4 + (\beta_1 + \beta_1) T^5 x^2 + v/L} dx + \kappa_2 \qquad (1)$$
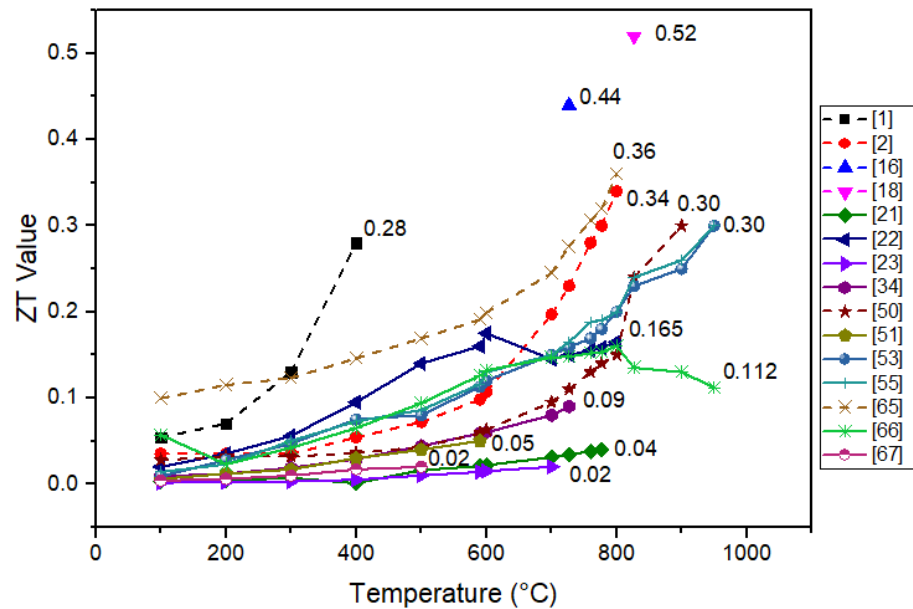
Figure 2. Comparison of nanostructuring and non-nanostructuring approach on the ZT value of ZnO ceramics over temperature.

C is an arbitrary constant in the Callaway equation which can be expressed as:

$$C = \frac{k_\beta}{2\pi^2 v} \left(\frac{k_\beta}{h} \right) \qquad (2)$$

and *x* can be expressed as:

$$x = \frac{h\omega}{k_\beta T} \qquad (3)$$

The key parameters can be found in Refs. [15,68,69]. For ZnO nanostructured thermo-electric materials, *L* can be deduced as the grain size of the nanostructures; thus, the smaller the grain size (*L* values), the lower the thermal conductivity (*κ*) of the nanostructure.

In the case of small, refined ZnO nanograins, a simultaneous increase in both phonon scattering and electron scattering can reduce the value of PF [2,65,70]. Nevertheless, the nanostructuring approach can successfully achieve higher ZT values compared to the non-nanostructuring approach, as illustrated in Figure 2. The highest reported ZT value from the nanostructuring approach was 0.52 at 827 °C [18], which is 42% higher than the best ZT value reported by its non-nanostructuring counterparts, 0.30 at 1000 °C [53,55]. At a lower temperature of 727 °C, the nanostructuring approach demonstrated a 62.5% higher ZT value compared to nanoparticles obtained from non-nanostructuring approaches [55]. Furthermore, the nanostructuring approach is capable of reaching a higher ZT value at a lower temperature than the non-nanostructuring approach. For instance, nanostructuring approach yielded a ZT value of 0.44 at 727 °C [16] and 0.3 at 777 °C [2], 950 °C [50] and 760 °C [65] compared to non-nanostructured approach which required 1000 °C [53,55]. This observation is in agreement with the Callaway model, where the larger grain size obtained from the non-nanostructuring approach resulted in higher thermal conductivity, whereby the corresponding ZT value was reduced, affecting its overall thermoelectric properties [71]. It can also be observed that ZnO nanoparticles demonstrated increasing ZT values at

higher temperatures attributed to the temperature-dependency of ZnO grain size. Higher temperatures yielded smaller ZnO grains, favouring the ZT value and thermoelectric properties [72].

At present, the high thermal conductivity of ZnO remains a major challenge in restricting its usage in thermoelectric applications. As mentioned earlier, higher thermal conductivity in ZnO ceramics is caused by higher phonon frequency, attributing to the ionic bonding and low atomic mass of ZnO lattice [70]. Moreover, the parameters affecting ZnO's thermal conductivity values are complex (e.g. carrier concentration, electrical conductivity, grain size, etc.). Such complexity remains an obstacle in realising ZnO-based thermoelectric materials. Fundamentally, the thermal conductivity (κ) of ZnO nanoparticles can be expressed as the sum of two portions, phonons and electric charge carriers, as referred to in equation $\kappa = \kappa_{lat} + \kappa_{ele}$ [24], where κ_{lat} is the lattice thermal conductivity that arises from heat transport phonon conducted through the crystal lattice and κ_{ele} is the electron thermal conductivity that arises from a heat-carrying charge carrier moving through the crystal structure [24]. The lattice thermal conductivity is influenced by the mass of the unit cell and the grain size [13]. Based on the equation, reducing the lattice thermal conductivity will enhance the ZT value, but reducing the electron thermal conductivity will exhibit little or no improvement in ZT values [50,73]. Thus, lowering the lattice thermal conductivity of ZnO can achieve outstanding thermoelectric properties.

On the other hand, the lower thermal conductivity of ZnO is due to the phonon scattering at grain boundaries [74]. Thus, refining grain sizes and the control over nano-microstructures of ZnO can reduce its thermal conductivity and align well with the Callaway model [8,15,21,27,75]. However, refining grain size also increases the electron scattering and reduces the value of the PF [70,76]. Since smaller grain size yields a higher abundance of grain boundaries, lattice misalignment at grain boundaries will induce phonon scattering. Consequently, lower thermal conductivity is achieved with more electron scattering; hence, PF is reduced [77,78]. Nevertheless, several studies suggested that the reduction of grain size down to <100 nm reduces the thermal conductivity and improves the ZT values [2,15,16]. In addition, other strategies, such as the development of novel materials with unique lattice vibrational modes, have also been reported [27,79].

Despite reports on novel material development [79], the research community has emphasised refining grain size to lower the thermal conductivity of ZnO. Figure 3 illustrates the relationship between grain size and thermal conductivity on ZT value using non-nanostructuring and nanostructuring approaches. The solid lines in the graph represent the non-nanostructuring approach [21,34,51,67,80], while the dashed lines [1,2,16,18,50] the nanostructuring approach. Based on the graph, ZnO nanoparticles demonstrated lower thermal conductivity and smaller grain size when synthesised using the nanostructuring approach compared to their non-nanostructuring counterparts. According to Kinemuchi et al. [70], it can be computed using the Callaway formula that the thermal conductivity of ZnO nanocomposite was >5 W/mK at high temperature when the grain size was reduced to <100 nm [74]. This observation is in line with Figure 3, where the grain size of >100 nm resulted in lower thermal conductivity and higher ZT values.

Biswas et al. synthesised 1 at% Al with 1.5 wt % RGO into ZnO using the solvothermal method [18]. It has s been found to show significant improvement in ZT value of 0.52 at 1100 K, which is an order of magnitude larger compared to that of bare undoped ZnO. The minimum crystallite size obtained is ~20 nm, and the thermal conductivity was 2.96 W/mK at 1100 K. Jood et al. [16] reported a high ZT value of 0.44 at 727 °C for $Zn_{0.975}Al_{0.025}O$ via rapid and scalable microwave-activated aminolytic decomposition of zinc and aluminium salts. This method produces a ZnO grain size of 15 nm and a particle size of $\leq$ 25 nm. The thermal conductivity measured at 300 K was 1.5 W/mK and was 2 W/mK at 1000 K. The obtained thermal conductivity was ~96% lower than the 49 W/mK in the bulk ZnO sample. This thermal conductivity can be attributed to the increase in phonon scattering at ZnO nanograin promoted by Al-induced grain refinement and Zinc Aluminate ($ZnAl_2O_4$) nano precipitates. Additionally, Zhang et al. [65] reported that micro/nanostructured

$Zn_{0.98}Al_{0.02}O$ could be successfully fabricated via hydrothermal synthesis and spark plasma sintering. The effective scattering on the boundaries and interfaces reduced the thermal conductivity value to $\kappa = 2.1$ W/mK at 1073 K, leading to a high ZT value, 0.36 at 1073 K.
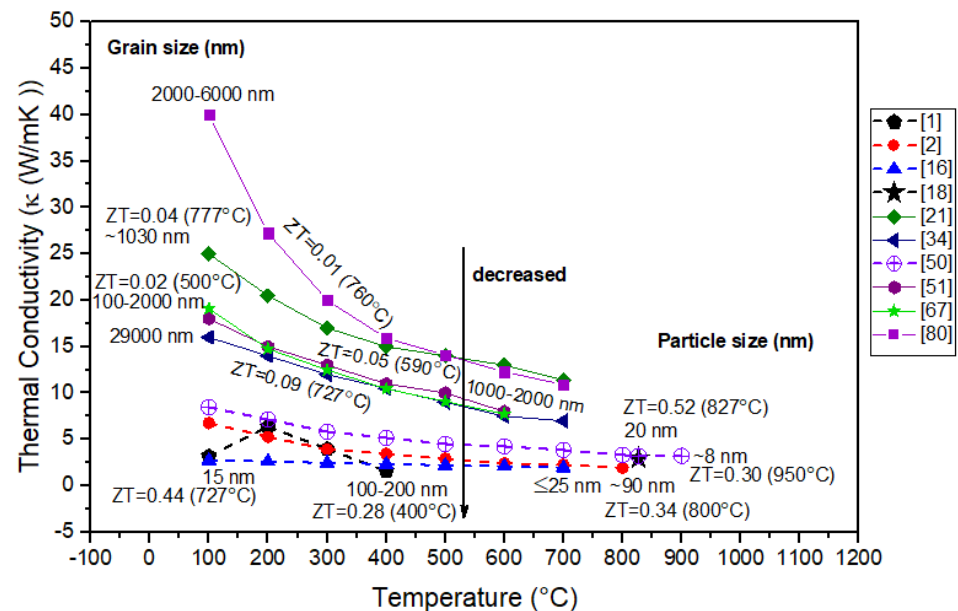
Figure 3. Effects of grain size on the thermal conductivity of ZnO ceramics at different temperatures.

Meanwhile, Nam et al. [2] reported a ZT value of 0.34 at 1073 K from the synthesised $Zn_{0.98}Al_{0.02}O$. The synthesis method used in the study was the nanostructuring approach involving a hybrid solution method and spark plasma sintering. The average ZnO grain size of ~90 nm was obtained. In addition to the ZT value of 0.34, the thermal conductivity was successfully reduced to 7.6 W/mK at room temperature, as it decreased with increasing temperature (κ_{700K} was ~3.2 W/mK and κ_{1000K} was < 2.0 W/mK). The thermal conductivity is reduced due to increasing phonon scattering at nanograin boundaries and nano precipitates. It also substantiated the observations in Figures 2 and 3, where the nanostructuring approach yielded ZnO nanocomposites with higher ZT values compared to the non-nanostructuring approach.

On the other hand, Han et al. [50] reported on the Al-doped ZnO nanoparticles using a forced-hydrolysis method. According to the study, ZnO ceramics were successfully produced with ZT values of 0.3 at 1223 K. The high ZT value was attributed to the low thermal conductivity of 3.2 W/mK at 1223 K, resulting from the nanostructuring of ZnO ceramics. The ZnO grain size that was obtained was ~8 nm, which was significantly smaller than the other Al-doped ZnO thermoelectrics reported by Jood et al. [16] and Nam et al. [2]. Meanwhile, Jantrasee et al. [1] reported a ZT value of 0.28 at 673 K of $Zn_{0.97}Al_{0.03}O$ synthesised using the hydrothermal method of zinc and aluminium salts. The nanostructuring approach yielded a ZT value of 1.59 W/mK with 100–200 nm grain size.

Based on the discussion above, it can be deduced that smaller grain size yields lower thermal conductivity in ZnO, leading to higher ZT values and favourable thermoelectric properties. Moreover, the nanostructuring approach yielded a smaller ZnO grain size than the non-nanostructuring approach, which resulted in lower thermal conductivity and higher ZT values. Additionally, doping of foreign particles (e.g. Al particles) can also effectively refine ZnO grain growth, resulting in smaller grain size. The next section discusses the effects of particle doping on ZnO's thermal conductivity and thermoelectric properties.

3.2. Doping Approach

Doping is another approach used to increase the ZT value of ZnO by increasing the carrier density [14,53,81] and refining its grain size. It is a process of adding impurities

in minimal quantities to intrinsic semiconductors to alter their behaviour or physical properties. Fundamentally, the Seebeck coefficient can be expressed by Joker relation as:

$$S = ATm^* \left(\frac{\pi}{3n} \right)^{\frac{2}{3}} \tag{4}$$

Meanwhile, the electrical conductivity of the thermoelectric materials can be expressed as:

$$\sigma = ne\mu \tag{5}$$

The definitions of the key parameters can be found in Ref. [82]. As the electrical conductivity (σ) and the Seebeck coefficient (S) are both a function of the carrier concentration (n), it can be deduced that higher carrier concentration leads to higher electrical conductivity but lower Seaback coefficient. Thus, an optimal doping condition is required to obtain optical thermoelectric properties from ZnO nanoparticles [83].

In achieving optimal doping conditions, selecting the appropriate doping elements to improve the carrier concentration by altering their electronic band structure [59] and electron transport properties [20] are important. At the same time, its Seebeck coefficient for optimal thermoelectric performances should also be retained. Meanwhile, undoped ZnO usually contains various intrinsic defects [84]. These intrinsic defects can significantly affect the electrical properties and thermoelectric performances of ZnO [84]. In this section, the dopings of ZnO and their resulting thermoelectric properties are briefly discussed. Based on the review, it can be observed that Al-doped ZnO and Gallium-doped ZnO demonstrated the best thermoelectric performances due to the high stability and distinguished thermopower [1]. The aluminium (Al) and gallium (Ga) dopants in ZnO increased the electrical conductivity of ZnO, thereby enhancing its thermoelectric performances [40].

3.2.1. Al-doped ZnO

Al is a cheap, durable, abundant, non-toxic and a common n-type donor dopant for ZnO [40]. The incorporation of Al into ZnO can reduce grain size and thermal conductivity without deteriorating its electrical conductivity and Seebeck coefficient. When Al is doped into ZnO, the additional enhancements in electrical properties on the existing high electron transport properties of ZnO result in outstanding thermoelectric performance [84]. Since the radius of Al atoms is smaller than Zn atoms, Zn atoms in ZnO lattice are easily displaced by Al dopant. As the name implied, Al atoms are n-type donor dopants. Thus, an additional free electron is obtained per lattice, which enhances the overall electrical conduction of Al-doped ZnO. Apart from the dopant effects, the covalent bond of the metal-to-oxygen bond in the oxide also contributes to the outstanding thermoelectric performance of Al/ZnO by improving carrier density and carrier mobility [40,53,55,66,85].

Table 1 summarises the thermoelectric properties of Al-doped ZnO. It can be deduced that Al-doped ZnO demonstrated improved thermoelectric performance [1,21,53,66,67,80]. The addition of small atomic percentages (1 to 3 at.%) of Al significantly improved the ZT value of ZnO compared with the undoped ZnO. However, the ZT value was still low and unsatisfactory [67]. The highest ZT value obtained was 0.44, which is insufficient for thermoelectric applications [16]. Furthermore, due to the presence of n-type dopant, the Seebeck coefficient exhibited a negative value within the investigated temperature range [16,80]. Apart from the improvements in the Seebeck coefficient, some results exhibited lower Seebeck coefficients upon Al doping [53,66,67]. This observation aligns with the Joker relation, where additional charge carriers in Al-doped ZnO reduce the Seebeck coefficient. Nevertheless, Al-doped ZnO improved electrical conductivity by introducing additional charge carriers. It is reflected from the metallic behaviour [21,53,66] of Al-doped Zn, which improves its electrical conductivity [16,53,66,67]. As ZnO is doped with Al at >3 at.% (near solubility limit), its resistivity is further reduced [22]. Despite the reduction in the Seebeck coefficient, the increase in electrical conductivity indicated readily allowable electric charge movement favouring the thermoelectric performance of ZnO [86].

Table 1. Thermoelectric properties of Al-doped ZnO.

Composition/Synthesis Method	Thermoelectric Properties	Ref
$(Zn_{0.99}Al_{0.01})O$/Solution combustion	ZT = 0.05, S = ~-148 µV/K, σ = ~21,000 S/m, PF = ~48,000 W/mK^2, κ = 8 W/mK at 590 °C	[51]
ZnO/RF plasma powder	ZT = ~0.007, S = ~-386 µV/K, σ = ~369 S/m, PF = ~0.55×10^{-4} W/mK^2, κ = 8 W/mK at 777 °C	[21]
$(Zn_{0.99}Al_{0.01})O$/RF plasma powder	ZT = 0.04, S = -68 µV/K, σ = ~86,505 S/m, PF = ~4×10^{-4} W/mK^2, κ = 10.6 W/mK at 777 °C	
$(Zn_{0.98}Al_{0.02})O$/Solid-state reaction	ZT = 0.3, S = -180 µV/K, σ = 40,000 S/m, κ = 5.4 W/mK at 1000 °C	[55]
ZnO/Nylon-lined ball mill	ZT = 0.028, S = -318 µV/K, σ = ~2037 S/m, PF = ~2.06×10^{-4} W/mK2, κ = 8 W/mK at 800 °C	[53,66]
$(Zn_{0.98}Al_{0.02})O$/Nylon-lined ball mill	ZT = 0.3, S = -182 µV/K, σ = ~39,971 S/m, PF = ~13.24×10^{-4} W/mK^2, κ = 5 W/mK at 1000 °C	
$(Zn_{0.98}Al_{0.02})O$/Solution method	ZT = 0.34, S = ~-148 µV/K, σ = ~29,000 S/m, κ = ~2 W/mK at 800 °C	[2]
$(Zn_{0.98}Al_{0.02})O$/Forced hydrolysis method	ZT = ~0.3, S = ~-205 µV/K, σ = ~18,798 S/m, κ = ~3.2 W/mK at 950 °C	[50]
ZnO/Solid-state reaction	ZT = ~0.009, S = ~-107 µV/K, σ = ~2500 S/m, κ = ~3.1 W/mK at 700 °C	[80]
$(Zn_{0.98}Al_{0.02})O$/Solid-state reaction	ZT = ~0.031, S = ~-133 µV/K, σ = 5400 S/m, κ = ~3 W/mK at 700 °C	
$(Zn_{0.975}Al_{0.025})O$/microwave synthesis	ZT = 0.44, S = ~-300 µV/K, σ = ~10,000 S/m κ = ~2 W/mK at 727 °C	[16]
ZnO/Sol-gel method	ZT = ~0.007, S = -240 µV/K, σ = ~1563 S/m, κ = ~9.8 W/mK at 500 °C	[67]
$(Zn_{0.97}Al_{0.03})O$/Sol-gel method	ZT = ~0.02, S = ~-81 µV/K, σ = ~37,500 S/m, κ = ~9.5 W/mK at 500 °C	
ZnO/Chemical co-deposition method	ZT = ~0.009, S = ~-250 µV/K, σ = ~1333 S/m, κ = ~8.3 W/mK at 600 °C	[22]
$(Zn_{0.97}Al_{0.03})O$/Chemical co-deposition method	ZT = 0.15, S = ~-240 µV/K, σ = ~15,000 S/m, κ = ~5 W/mK at 600 °C	

The thermal conductivity of ZnO is higher at room temperature (40 W/mK) and decreases with the increase of temperature, 5 W/mK at 1000 °C [53]. The high thermal conductivity of ZnO can be attributed to its lattice structure [53]. Upon Al doping, the thermal conductivity decreases with the increasing amount of Al added due to the enhancement of the phonon scattering at nanograin boundaries and nano precipitates [2,67]. Moreover, the increase in the Al contents may cause random disorder phonon scattering induced by Al deficient sites [67]. Hence, thermal conductivity is lowered, resulting in enhanced thermoelectric performances [51].

3.2.2. Ga-doped ZnO

Ga is in group III of the periodic table, akin to aluminium and indium. Through Ga doping, the carrier concentration and electron and point defect concentration are increased, subsequently increasing electrical conductivity and decreasing thermal conductivity [78]. Table 2 summarises the thermoelectric properties of ZnO doped with Ga at different temperatures. Based on Table 2, it can be deduced that the addition of Ga into ZnO improved the electrical conductivity. Simultaneously, the Seebeck coefficient of Ga-doped ZnO also increased due to the presence of the voids, despite the additional charge carriers, according to Joker relation. Apart from that, as suggested by Jood et al. [16], the voids reduce the thermal conductivity of ZnO by increasing phonon scattering centres, enhancing the thermoelectric performances of ZnO.

Table 2. Thermoelectric properties of Ga-doped ZnO.

Composition/Synthesis Method	Thermoelectric Properties	Ref
ZnO/Nylon-lined ball mill	ZT = ~0.076, S = ~−430 μV/K, σ = ~1622 S/m, PF = ~3 × 10^{-4} W/mK^2, κ = 5 W/mK at 1000 °C	[66]
$(Zn_{0.98}Ga_{0.02})$O/Nylon-lined ball mill	ZT = ~0.13, S = ~−180 μV/K, σ = ~16,600 S/m, PF = ~5.38 × 10^{-4} W/mK^2, κ = 5 W/mK at 1000 °C	
$(Zn_{0.995}Ga_{0.005})$O/high energy wet milling	ZT = ~0.0022, S = ~−133 μV/K, σ = ~10,989 S/m, κ = 26.9 W/mK at 27 °C	[87]
ZnO/Wet chemistry gel combustion method	ZT = ~0.0022, S = ~−312.5 μV/K, σ = ~197 S/m, κ = ~9.4 W/mK at 800 °C	[78]
$(Zn_{0.98}Ga_{0.02})$O/Wet chemistry gel combustion method	ZT = ~0.026, S = ~−562.5 μV/K, σ = ~268 S/m, κ = ~3.5 W/mK at 800 °C	
$(Zn_{0.99}Ga_{0.01})$O/Atomic layer deposition	S = 60 μV/K, σ = ~180,832 S/m, PF = ~6.6 × 10^{-4} W/mK^2	[88]

3.2.3. Ni-doped ZnO

Nickel (Ni) belongs to group 10 (transition metals) in the periodic table. It is very hard, ductile and has high thermal conductivity (90.9 W/mK). Ni dopant acts as an excellent electron donor, as their presence decreases the charge carrier concentration in ZnO [23]. The primary material used in Ni-doping is Nickel oxide (NiO), which has a cubic structure [34,46]. Table 3 indicates the thermoelectric properties of Ni-doped ZnO. The addition of Ni to ZnO with the composition $Zn_{1-x}Ni_xO$ (x = 0.03) indicates the optimal value of ZT at the higher temperature. ZT value reduces as the composition increases above x = 0.03. The average size of samples is smaller (17.1 to 5.1 μm) with higher Ni content [46]. Nevertheless, this method produced an average ZnO grain size of 28 nm for intrinsic ZnO, where the grain size was reduced to 26 nm for Ni-doped $(Zn_{0.97}Ni_{0.03})$O powder [34]. Meanwhile, Ni-doped ZnO with the composition of x < 0.03 demonstrated a dense microstructure of a single-phase wurtzite ZnO structure [23,34] and a secondary phase as cubic when the composition x > 0.0325. Despite the reduction in thermal conductivity associated with grain size reduction, the charge mobility in the grain boundaries decreases due to the pinning effects. This observation exhibits a trade-off in Ni-doped ZnO thermoelectric materials [46].

Table 3. Thermoelectric properties of Ni-doped ZnO.

Composition/Synthesis Method	Thermoelectric Properties	Ref
ZnO/Precipitation $(Zn_{0.97}Ni_{0.03})$O/Precipitation	ZT = 0.002, S = ~−517 μV/K, σ = ~50 S/m, κ = 8 W/mK at 700 °C ZT = 0.02, S = ~−306 μV/K, σ = ~1790 S/m, κ = 8 W/mK at 700 °C	[23]
ZnO/Tape casting method $(Zn_{0.97}Ni_{0.03})$O/Tape casting method	PF = 0.62 × 10^{-4} W/mK^2, S = ~−203 μV/K, σ = ~1500 S/m at 800 °C PF = 17.6 × 10^{-4} W/mK^2, S = −503 μV/K, σ = 6970 S/m at 800 °C	[46]
ZnO/Liquid route synthesis	ZT = 0.0034, S = ~−310 μV/K, σ = ~250 S/m, PF = ~0.24 × 10^{-4} W/mK^2, κ = 7 W/mK at 727 °C	[34]
$(Zn_{0.97}Ni_{0.03})$O/Liquid route synthesis	ZT = 0.09, S = ~−420 μV/K, σ = ~3401 S/m, PF = 6 × 10^{-4} W/mK^2, κ = 6.5 W/mK at 727 °C	

Among the reported ZT values of Ni-doped ZnO thermoelectric materials, Colder et al. [34] reported the highest value of 0.09, which was 75% higher compared to the value reported by Koresh and Amouyal [23]. Similar to Al-doped ZnO, the Seebeck coefficients reported here were also negative values, indicating n-type conduction [23,34,46]. According to Koresh and Amouyal, higher Ni composition resulted in higher Seebeck coefficient values at x < 0.03 [34,46], whereby increased Ni composition will result in reduced Seebeck coefficient, x > 0.03 [23]. Furthermore, the electrical conductivity of ZnO was also increased upon Ni doping, primarily due to the increasing electron carrier

concentration [34]. Similar to the Seebeck coefficient, when the Ni composition reaches $x >$ 0.03, the electrical conductivity begins to decrease [46]. This phenomenon could be due to the occurrences of the secondary phase in the vicinity of the grain boundary, which in turn, decreases the grain size. Smaller grain sizes yield a higher abundance of high resistivity grain boundary, resulting in low electrical conductivity [34,46]. Apart from the electrical conductivity, the Ni-doped element is capable of reducing the thermal conductivity at room temperature [25]. However, despite the changes in electrical conductivity, the overall value of thermal conductivity does not differ much with the addition of Ni in ZnO samples at higher temperatures [23,34,46].

3.2.4. Bi-doped ZnO

Bismuth (Bi) belongs to group 15 in the periodic table. It has relatively lower toxicity among heavy metals and low thermal conductivity (7.97 W/mK). Guan et al. [80] investigated the effects of bismuth (III) oxide (Bi_2O_3) doped in ZnO. The samples were prepared using a solid-state reaction method that yielded grain size within the range of 2 to 6 μm. The Bi_2O_3 particles in ZnO were segregated at the grain boundaries level resulting in their low solubility. It was also reported that the low melting point of Bi_2O_3 in ZnO at grain boundaries affects the grain growth in Bi-doped ZnO samples by transport accelerations.

The addition of Bi in ZnO demonstrated a dramatic increase in the Seebeck coefficient values (−533 μV/K). However, the electrical conductivity decreased beyond this value owing to higher electrical resistivity (>10^8 Ω). Moreover, it is worth noting that the carrier concentration is also lower than that of Al-doped ZnO. Apart from the electrical conductivity, the addition of Bi in ZnO significantly improved its lattice thermal conductivity intrinsic ZnO. Based on the significant increase in grain size due to the segregation of Bi_2O_3, it can be suggested that Bi is not an ideal dopant to improve the ZT value of ZnO for thermoelectric applications. Table 4 illustrates the thermoelectric properties of Bi-doped in ZnO.

Table 4. Thermoelectric properties of Bi-doped ZnO.

Composition/Synthesis Method	Thermoelectric Properties	Ref
ZnO/Solid-state reaction ($Zn_{0.98}Bi_{0.02}$)O/Solid-state reaction	ZT = ~0.009, S = ~−107 μV/K, σ = ~2500 S/m, κ = ~3.1 W/mK at 700 °C ZT = 0.006, S = −533 μV/K, σ = ~230 S/m, κ = 10.5 W/mK at 700 °C	[80]

3.2.5. Sn-doped ZnO

Tin (Sn) belongs to group 14 of the periodic table, where it has low toxicity and is soft and ductile with a thermal conductivity value of 66.8 W/mK. Table 5 indicates the effects of tin (IV) oxide (SnO_2) doped in ZnO ($Zn_{1-x}Sn_xO$) on its thermoelectric properties. The average grain size obtained ranged from 13.9 to 3.5 μm. However, with higher Sn doping concentrations, the grain size is reduced [38]. This reduction can be attributed to the pinning effect caused by Zn_2SnO_4 particles present at the grain boundaries of ZnO, along with the dragging effects between the added SnO_2 and grain boundaries. These effects result in lower electron mobility by reducing grain size [38]. Meanwhile, Guan et al. [80] also reported lower mobility in Sn-doped ZnO samples caused by the increased ionised impurities scattering within the samples.

Table 5. Thermoelectric properties of Sn-doped ZnO.

Composition/Synthesis Method	Thermoelectric Properties	Ref
($Zn_{0.99}Sn_{0.01}$)O/Solid-state reaction	PF = 1.25×10^{-3} W/mK^2, S = ~−160 μV/K, σ = ~15 S/m at 800 °C	[38]
ZnO/Solid-state reaction ($Zn_{0.98}Sn_{0.02}$)O/Solid-state reaction	ZT = ~0.009, S = ~−107 μV/K, σ = ~2500 S/m, κ = ~3.1 W/mK at 700 °C ZT = 0.012, S = −93 μV/K, σ = 900 S/m, κ = 7 W/mK at 700 °C	[80]

The electrical conductivity for undoped ZnO increases slightly with the increment of temperature, indicating its inherent semiconductor behaviour [38]. However, the addition

of Sn in ZnO modified the semiconductor conduction behaviour of intrinsic ZnO, where the electric conductivity of Sn-doped ZnO decreases with increasing temperature [38]. The electrical conductivity behaviour of Sn-doped ZnO observed by Guan et al. [80] exhibited the opposite trend from other dopants (Ni, Al, etc.). As the electrical conductivity increases, the Seebeck coefficient value reduces, leading to a lower ZT value attributed to the lattice structure of Sn dopants. Since Sn has twice the ionised donor impurity that provides carriers (electrons) [80], the addition of Sn content increases the carrier concentration compared to Al, Bi, Ni and undoped ZnO [80]. This observation aligned with the Joker relation, where a higher number of charge carriers result in higher electrical conductivity and a lower Seebeck coefficient.

The addition of small amounts of SnO_2 leads to a strong donor effect [38,80]. Zn atoms (Zn^{2+}) in the ZnO lattice can be easily substituted by Sn atoms (Sn^{4+}), whereby the lattice distortion is not affected. This differs from the Al dopant discussed in the previous section. Since Zn and Sn have similar radii, Sn dopant can substitute vacancies in ZnO lattice without creating significant voids or defects [38,80]. In terms of the alteration of thermoelectric properties, the addition of Sn increases the thermal conductivity due to the larger grain size leading to decreased phonon scattering.

4. Concluding Remarks

ZnO possesses promising potential in thermoelectric application due to its high physicochemical stability, tunable properties and high abundance, which subsequently yields low synthesis cost and complexity. The overall effect is a ZnO thermoelectric device can operate at higher temperatures, has higher conversion efficiency, has higher reliability and costs less to produce. With this research, millions of money in savings or in new opportunities to recover waste heat from high-temperature processes could be made available. In order to enhance its thermoelectric properties, several approaches can be employed: (i) lowering the thermal conductivity, (ii) increasing the Seebeck coefficient, and (iii) increasing the electrical conductivity. Based on the Hallaway model, smaller grain size ZnO is desired to achieve lower thermal conductivity. In order to improve the electrical conductivity of ZnO, a higher number of charge carriers is needed. However, based on the Joker relation on the Seebeck coefficient of ZnO, a high number of charge carriers result in lowered Seebeck coefficient in ZnO, negatively affecting the overall thermoelectric properties of ZnO. Therefore, optimisation of charge carriers in ZnO is needed to obtain the desired thermoelectric properties.

According to the extant literature, several strategies have been reported to enhance the thermoelectric properties of ZnO, including nanostructuring synthesis technique and doping. Between the nanostructuring and non-nanostructuring synthesis approaches, the nanostructuring approach yielded a smaller grain size corresponding to lower thermal conductivity and improved Seebeck coefficient corresponding to its thermoelectric properties. As for doping strategies, doping of foreign particles in ZnO improves the overall thermoelectric properties via several mechanisms. Firstly, the inclusion of foreign particles (such as Al) inhibits the grain growth, and the combination in the ZnO lattice results in low thermal conductivity. Meanwhile, the addition of charged particles increased the electrical conductivity of ZnO. These mechanisms effectively improved the thermoelectric properties of ZnO. However, above the optimal doping concentration, the excessively high number of charge carriers will reduce the Seebeck coefficient of ZnO, affecting its overall thermoelectric properties. Thus, optimal doping conditions are called for.

5. Way Forward

This section is not mandatory but may be added if there are patents resulting from the work reported in this manuscript. The review addressed the preliminary understanding of the effects of doping and nanostructuring on the thermoelectric properties of ZnO. The reported state-of-the-art strategy demonstrated the individual impact of doping concentration, doping species and nanostructuring strategies on the Seebeck coefficient, electrical

conductivity and thermal conductivity of ZnO thermoelectric materials. Therefore, several technical gaps should be focused on to fully utilise ZnO materials for commercial thermoelectric devices. First are the effects of hybrid doping species. Each doping species possess individualised advantages and drawbacks. For instance, Al dopant introduces increased carrier concentration without trading off the Seebeck coefficient. Meanwhile, Sn dopant resulted in a relatively higher enhancement in electrical conductivity, but the presence of excessive charge carriers lowered the Seebeck coefficient. A hybridised doping of Al and Sn species can yield promising outcomes in the thermoelectric properties of ZnO.

Apart from the mixed doping species, another approach which can be attempted is the mixture of nanostructuring and doping strategies. Nanostructuring refines the grain size of ZnO to achieve low thermal conductivity and to enhance its corresponding thermoelectric properties. Meanwhile, doping of ZnO suppresses the growth of ZnO grains, enhancing its electrical properties by reducing the Seebeck coefficient. It can be speculated that these two strategies can complement each other to potentially enhance the thermoelectric performance of ZnO to another level. In order to achieve the desired properties, this review provides a preliminary understanding of the nanostructuring and doping of ZnO thermoelectric materials, which also serves as a useful fundamental for further developments of ZnO-based thermoelectric technologies.

Author Contributions: Conceptualisation (idea and realization), S.S.; review of the state of the art, S.S.; writing—original draft preparation, S.S.; visualisation, S.S.; writing—review and editing, S.S., I.S., U.M.B.A.-N. and M.F.O.; formal analysis, S.S.; supervision, S.S.; funding acquisition, S.S. All authors have read and agreed to the published version of the manuscript.

Funding: This research was funded by UMP-IIUM-UiTM Sustainable Research Collaboration 2020 grant number RDU200744.

Acknowledgments: The authors would like to acknowledge generous support from the School of Mechanical Engineering, Faculty of Engineering, Universiti Teknologi Malaysia, Faculty of Science, Universiti Teknologi Malaysia, Faculty of Manufacturing and Mechatronic Engineering Technology, Universiti Malaysia Pahang and UMP-IIUM-UiTM Sustainable Research Collaboration 2020 (RDU200744).

Conflicts of Interest: The authors declare no conflict of interest.

References

1. Jantrasee, S.; Moontragoon, P.; Pinitsoontorn, S. Thermoelectric properties of Al-doped ZnO: Experiment and simulation. *J. Semicond.* **2016**, *37*, 092002-1–092002-8. [CrossRef]
2. Nam, W.H.; Lim, Y.S.; Choi, S.-M.; Seo, W.-S.; Lee, J.Y. High-temperature charge transport and thermoelectric properties of a degenerately Al-doped ZnO nanocomposite. *J. Mater. Chem.* **2012**, *22*, 14633–14638. [CrossRef]
3. Ihns, M. Structural Engineering of $Ca_3Co_4O_9$ Thermoelectric Thin Films. Master's Thesis, University of Twente, Enschede, The Netherlands, 2013.
4. Zaferani, S.H.; Jafarian, M.; Vashaee, D.; Ghomashchi, R. Thermal Management Systems and Waste Heat Recycling by Thermoelectric Generators—An Overview. *Energies* **2021**, *14*, 5646. [CrossRef]
5. Fergus, J.W. Oxide materials for high temperature thermoelectric energy conversion. *J. Eur. Ceram. Soc.* **2012**, *32*, 525–540. [CrossRef]
6. Zhu, B.B.; Li, D.; Zhang, T.S.; Luo, Y.B.; Donelson, R.; Zhang, T.; Zheng, Y.; Du, C.F.; Wei, L.; Hng, H.H. The improvement of thermoelectric property of bulk ZnO via ZnS addition: Influence of intrinsic defects. *Ceram. Int.* **2018**, *44*, 6461–6465. [CrossRef]
7. Funahashi, R.; Barbier, T.; Combe, E. Thermoelectric materials for middle and high temperature ranges. *J. Mater. Res.* **2015**, *30*, 2544–2557. [CrossRef]
8. Koumoto, K.; Wang, Y.; Zhang, R.; Kosuga, A.; Funahashi, R. Oxide Thermoelectric Materials: A Nanostructuring Approach. *Annu. Rev. Mater. Res.* **2010**, *40*, 363–394. [CrossRef]
9. Jouharaa, H.; Zabnienska-Góra, A.; Khordehgaha, N.; Doraghia, Q.; Ahmada, L.; Normana, L.; Axcella, B.; Wrobela, L.; Daid, S. Thermoelectric generator (TEG) technologies and applications. *Int. J. Thermofluids.* **2021**, *9*, 100063. [CrossRef]
10. Huang, S.; Ning, S.; Xiong, R. First-Principles Study of Silicon–Tin Alloys as a High-Temperature Thermoelectric Material. *Materials* **2022**, *15*, 4107. [CrossRef] [PubMed]
11. Wang, H.; Liang, X.; Wang, J.; Jiao, S.; Xue, D. Multifunctional inorganic nanomaterials for energy applications. *Nanoscale* **2020**, *12*, 14–42. [CrossRef]

12. Ohtaki, M. Recent aspects of oxide thermoelectric materials for power generation from mid-to-high temperature heat source. *J. Ceram. Soc. Jpn.* **2011**, *119*, 770–775. [CrossRef]

13. Lourdes, M.G. Preparation and Characterisation of Nanostructured Bulk Bi$_2$Te$_3$ Thermoelectric Materials Using Ultrasound Milling. Ph.D. Thesis, Cardiff University, Cardiff, UK, 2016.

14. Yin, Y.; Tudu, B.; Tiwari, A. Recent advances in oxide thermoelectric materials and modules. *Vacuum* **2017**, *146*, 356–374. [CrossRef]

15. Sulaiman, S.; Izman, S.; Uday, M.B.; Omar, M.F. Review on grain size effects on thermal conductivity in ZnO thermoelectric materials. *RSC Adv.* **2022**, *12*, 5428–5438. [CrossRef]

16. Jood, P.; Mehta, R.J.; Zhang, Y.; Peleckis, G.; Wang, X.; Siegel, R.W.; Borca-tasciuc, T.; Dou, S.X.; Ramanath, G. Al-Doped Zinc Oxide Nanocomposites with Enhanced Thermoelectric Properties. *Nano. Lett.* **2011**, *11*, 4337–4342. [CrossRef] [PubMed]

17. Mohammed, M.A.; Sudin, I.; Noor, A.M.; Rajoo, S.; Uday, M.B.; Obayes, N.H.; Omar, M.F. A review of thermoelectric ZnO nanostructured ceramics for energy recovery. *Int. J. Eng. Technol.* **2018**, *7*, 27–30. [CrossRef]

18. Biswas, S.; Singh, S.; Singh, S.; Chattopadhyay, S.; Silva, K.K.H.D.; Yoshimura, M.; Mitra, J.; Kamble, V.B. Selective Enhancement in Phonon Scattering Leads to a High Thermoelectric Figure-of-Merit in Graphene Oxide-Encapsulated ZnO Nanocomposites. *ACS Appl. Mater. Interfaces* **2021**, *13*, 23771–23786. [CrossRef] [PubMed]

19. Chen, Z.; Shi, X.; Zhao, L.; Zou, J. High-performance SnSe thermoelectric materials: Progress and future challenge. *Prog. Mater. Sci.* **2018**, *97*, 283–346. [CrossRef]

20. Wiff, J.P.; Kinemuchi, Y.; Kaga, H.; Ito, C.; Watari, K. Correlations between thermoelectric properties and effective mass caused by lattice distortion in Al-doped ZnO ceramics. *J. Eur. Ceram. Soc.* **2008**, *29*, 1413–1418. [CrossRef]

21. Cheng, H.; Xu, X.J.; Hng, H.H.; Ma, J. Characterization of Al-doped ZnO thermoelectric materials prepared by RF plasma powder processing and hot press sintering. *Ceram. Int.* **2009**, *35*, 3067–3072. [CrossRef]

22. Qu, X.; Wang, W.; Lv, S.; Jia, D. Thermoelectric properties and electronic structure of Al-doped ZnO. *Solid State Commun.* **2011**, *151*, 332–336. [CrossRef]

23. Koresh, I.; Amouyal, Y. Effects of microstructure evolution on transport properties of thermoelectric nickel-doped zinc oxide. *J. Eur. Ceram. Soc.* **2017**, *37*, 3541–3550. [CrossRef]

24. Liu, W.; Hu, J.; Zhang, S.; Deng, M.; Han, C.-G.; Liu, Y. New trends, strategies and opportunities in thermoelectric materials: A perspective. *Mater. Today Phys.* **2017**, *1*, 50–60. [CrossRef]

25. Park, Y.; Cho, K.; Kim, S. Thermoelectric characteristics of glass fibers coated with ZnO and Al-doped ZnO. *Mater. Res. Bull.* **2017**, *96*, 246–249. [CrossRef]

26. Kedia, S.K.; Singh, A.; Chaudhary, S. Design, development, and testing of a thermopower measurement system by studying the electron transport properties on indium and nitrogen co-doped sputtered ZnO films. *Measurement* **2018**, *117*, 49–56. [CrossRef]

27. Zhou, X.; Yan, Y.; Lu, X.; Zhu, H.; Han, X.; Chen, G.; Ren, Z. Routes for high-performance thermoelectric materials. *Mater. Today* **2018**, *21*, 974–988. [CrossRef]

28. Zhou, B.; Chen, L.; Li, C.; Qi, N.; Chen, Z.; Su, X.; Tang, X. Significant Enhancement in the Thermoelectric Performance of Aluminum-Doped ZnO Tuned by Pore Structure. *ACS Appl. Mater. Interfaces* **2020**, *12*, 51669–51678. [CrossRef]

29. Wu, N. Development and Processing of p-Type Oxide Thermoelectric Materials. Ph.D. Thesis, Technical University of Denmark, Copenhagen, Denmark, 2014.

30. Tritt, T.M.; Subramanian, M. Thermoelectric Materials, Phenomena, and Applications: A Bird' s Eye View. *MRS Bull.* **2006**, *31*, 188–198. [CrossRef]

31. Markov, M.; Rezaei, S.E.; Sadeghi, S.N.; Esfarjani, K.; Zebarjadi, M. Thermoelectric properties of semimetals. *Phys. Rev. Mater.* **2019**, *3*, 095401. [CrossRef]

32. Kim, H.J.; Skuza, J.R.; Park, Y.; King, G.C.; Choi, S.H.; Nagavalli, A. System to Measure Thermal Conductivity and Seebeck Coefficient for Thermoelectrics. *NasaTM* **2012**, *217791*, LF99-15831.

33. Yamaguchi, H.; Chonan, Y.; Oda, M.; Komiyama, T.; Aoyama, T.; Sugiyama, S. Thermoelectric properties of ZnO ceramics Co-doped with Al and transition metals. *J. Electron. Mater.* **2011**, *40*, 723–727. [CrossRef]

34. Colder, H.; Guilmeau, E.; Harnois, C.; Marinel, S.; Retoux, R.; Savary, E. Preparation of Ni-doped ZnO ceramics for thermoelectric applications. *J. Eur. Ceram. Soc.* **2011**, *31*, 2957–2963. [CrossRef]

35. Brintha, S.R.; Ajitha, M. Synthesis and characterization of ZnO nanoparticles via aqueous solution, sol-gel and hydrothermal methods. *J. Appl. Chem.* **2015**, *8*, 66–72. [CrossRef]

36. Jurablu, S.; Farahmandjou, M.; Firoozabadi, T.P. Sol-Gel Synthesis of Zinc Oxide (ZnO) Nanoparticles: Study of Structural and Optical Properties. *J. Sci. Islamic Repub. Iran* **2015**, *26*, 281–285.

37. Wu, Z.-H.; Xie, H.-Q.; Zhai, Y.-B. Preparation and Thermoelectric Properties of Co-Doped ZnO Synthesized by Sol–Gel. *J. Nanosci. Nanotechnol.* **2015**, *15*, 3147–3150. [CrossRef] [PubMed]

38. Park, K.; Seong, J.K.; Kwon, Y.; Nahm, S.; Cho, W.S. Influence of SnO2addition on the thermoelectric properties of Zn1-xSnxO ($0.01 \leq x \leq 0.05$). *Mater. Res. Bull.* **2008**, *43*, 54–61. [CrossRef]

39. Kumar, M.; Sahu, S.S. Zinc Oxide Nanostructures Synthesized by Oxidization of Zinc. Master's Thesis, National Institute of Technology Rourkela, Rourkela, India, 2010.

40. Ilican, S.; Gorgun, K.; Aksoy, S.; Caglar, Y.; Caglar, M. Fabrication of p-Si/n-ZnO: Al heterojunction diode and determination of electrical parameters. *J. Mol. Struct.* **2018**, *1156*, 675–683. [CrossRef]

41. Kołodziejczak-Radzimska, A.; Jesionowski, T. Zinc Oxide—From Synthesis to Application: A Review. *Materials* **2014**, *7*, 2833–2881. [CrossRef] [PubMed]

42. Baghdadi, N.; Salah, N.; Alshahrie, A.; Koumoto, K. Microwave Irradiation to Produce High Performance Thermoelectric Material Based on Al Doped ZnO Nanostructures. *Crystals* **2020**, *10*, 610. [CrossRef]

43. Patel, N. Characterization of Electrical Performance of Aluminum-Doped Zinc Oxide Pellets. *DePaul Discov.* **2014**, *3*, 6.

44. Feng, Q.; Shi, X.; Xing, Y.; Li, T.; Li, F.; Pan, D.; Liang, H. Thermoelectric microgenerators using a single large-scale Sb doped ZnO microwires. *J. Alloy. Compd.* **2018**, *739*, 298–304. [CrossRef]

45. Morkoç, H.; Özgür, Ü. *Zinc Oxide: Fundamentals, Materials and Device Technology*; WILEY-VCH Verlag GmbH & Co. KGaA: Weinheim, Germany, 2009; ISBN 978-3-527-40813-9.

46. Park, K.; Seong, J.K.; Kim, G.H. NiO added Zn1-xNixO ($0 \leq x \leq 0.05$) for thermoelectric power generation. *J. Alloy. Compd.* **2009**, *473*, 423–427. [CrossRef]

47. Janotti, A.; Walle, C.G.V.D. Fundamentals of zinc oxide as a semiconductor. *Rep. Prog. Phys.* **2009**, *72*, 126501. [CrossRef]

48. Wojnarowicz, J.; Chudoba, T.; Lojkowski, W. A Review of Microwave Synthesis of Zinc OxideNanomaterials: Reactants, Process Parametersand Morphologies. *Nanomaterials* **2020**, *10*, 1086. [CrossRef] [PubMed]

49. Kumar, P.; Saini, M.; Singh, M.; Chhillar, N.; Dehiya, B.S.; Kishor, K.; Alharthi, F.A.; Al-Zaqri, N.; Alghamdi, A.A. Micro-Plasma Assisted Synthesis of ZnO Nanosheets for theEfficient Removal of Cr^{6+} from the Aqueous Solution. *Crystals* **2021**, *11*, 2. [CrossRef]

50. Han, L. High Temperature Thermoelectric Properties of ZnO Based Materials. Ph.D. Thesis, Technical University of Denmark, Copenhagen, Denmark, 2014.

51. Zhang, L.; Tosho, T.; Okinaka, N.; Akiyama, T. Thermoelectric Properties of Solution Combustion Synthesized Al-Doped ZnO. *Mater. Trans.* **2008**, *49*, 2868–2874. [CrossRef]

52. Sayari, A.; El Mir, L. Structural and optical characterization of Ni and Al co-doped ZnO nanopowders synthesized via the sol-gel process. *Kona Powder Part. J.* **2015**, *32*, 154–162. [CrossRef]

53. Tsubota, T.; Ohtaki, M.; Eguchi, K.; Arai, H. Thermoelectric properties of Al-doped ZnO as a promising oxide material for high-temperature thermoelectric conversion. *J. Mater. Chem.* **1997**, *7*, 85–90. [CrossRef]

54. Virtudazo, R.V.R.; Srinivasan, B.; Guo, Q.; Wu, R.; Takei, T.; Shimasaki, Y.; Wada, H.; Kuroda, K.; Bernik, S.; Mori, T. Improvement in the thermoelectric properties of porous networked Al-doped ZnO nanostructured materials synthesized via an alternative interfacial reaction and low-pressure SPS processing. *Inorg. Chem. Front.* **2020**, *7*, 4118–4132. [CrossRef]

55. Ohtaki, M.; Tsubota, T.; Eguchi, K.; Arai, H. High-temperature thermoelectric properties of $(Zn_{1-x}Al_x)O$. *J. Appl. Phys.* **1996**, *79*, 1816–1818. [CrossRef]

56. Prasad, K.S.; Rao, A.; Bhardwaj, R.; Johri, K.K.; Chang, C.; Kuo, Y. Spark plasma sintering technique: An alternative method to enhance ZT values of Sb doped Cu_2SnSe_3. *J. Mater. Sci. Mater. Electron.* **2018**, *29*, 13200–13208. [CrossRef]

57. Hedge, G.S.; Prabhu, A.N.; Huang, R.Y.; Kuo, Y.K. Reduction in thermal conductivity and electrical resistivity of indium and tellurium co-doped bismuth selenide thermoelectric system. *J. Mater. Sci. Mater. Electron.* **2020**, *31*, 19511–19525. [CrossRef]

58. Neeli, G.; Behara, D.K.; Kumar, M.K. State of the Art Review on Thermoelectric Materials. *Int. J. Sci. Res.* **2016**, *5*, 1833–1844. [CrossRef]

59. Gayner, C.; Kar, K.K. Recent advances in thermoelectric materials. *Prog. Mater. Sci.* **2016**, *83*, 330–382. [CrossRef]

60. Muthusamy, O.; Singh, S.; Hirata, K.; Kuga, K.; Harish, S.K.; Shimomura, M.; Adachi, M.; Yamamoto, Y.; Matsunami, M.; Takeuchi, T. Synergetic Enhancement of the Power Factor and Suppression of Lattice Thermal Conductivity via Electronic Structure Modification and Nanostructuring on a Ni- and B-Codoped p-Type Si–Ge Alloy for Thermoelectric Application. *ACS Appl. Electron. Mater.* **2021**, *3*, 5621–5631. [CrossRef]

61. Kavita; Gupta, V.; Ranjeet. Structural and morphological properties of nanostructured Bi2Te3 with Mn-doping for thermoelectric applications. *Mater. Today Proc.* **2021**, *54*, 820–826. [CrossRef]

62. Li, D.H.; He, S.F.; Chen, J.; Jiang, C.Y.; Yang, C. Solid-state Chemical Reaction Synthesis and Characterization of Lanthanum Tartrate Nanocrystallites under Ultrasonication Spectra. *IOP Conf. Ser. Mater. Sci. Eng.* **2017**, *242*, 012023. [CrossRef]

63. Yahya, N. *Carbon and Oxide Nanostructures: Synthesis, Characterisation and Applications*; Springer Link: Berlin/Heidelberg, Germany, 2011; ISBN 978-3-642-14673-2.

64. Jeevanandam, J.; Barhoum, A.; Chan, Y.S.; Dufresne, A.; Danquah, M.K. Review on nanoparticles and nanostructured materials: History, sources, toxicity and regulations. *J. Nanotechnol.* **2018**, *9*, 1050–1074. [CrossRef]

65. Zhang, D.-B.; Li, H.-Z.; Zhang, B.-P.; Liang, D.; Xia, M. Hybrid-structured ZnO thermoelectric materials with high carrier mobility and reduced thermal conductivity. *RSC Adv.* **2017**, *7*, 10855–10864. [CrossRef]

66. Tsubota, T.; Ohtaki, M.; Eguchi, K.; Arai, H. Thermoelectric properties of ZnO Doped with The Group 13 Elements. In Proceedings of the 16th International Conference on Thermoelectrics, Dresden, Germany, 26–29 August 1997; pp. 240–243. [CrossRef]

67. Cai, K.F.; Müller, E.; Drašar, C.; Mrotzek, A. Preparation and thermoelectric properties of Al-doped ZnO ceramics. *Mater. Sci. Eng. B Solid-State Mater. Adv. Technol.* **2003**, *104*, 45–48. [CrossRef]

68. Callaway, J. Model for Lattice Thermal Conductivity at Low Temperatures. *Phys. Rev.* **1959**, *113*, 1046–1051. [CrossRef]

69. Bui, C.T.; Sow, C.H.; Li, B.; Thong, J.T.L. Diameter-Dependent Thermal Transport in Individual ZnO Nanowires and its Correlation with Surface Coating and Defects. *Small* **2012**, *8*, 738–745. [CrossRef] [PubMed]

70. Kinemuchi, Y.; Nakano, H.; Mikami, M.; Kobayashi, K.; Watari, K.; Hotta, Y. Enhanced boundary-scattering of electrons and phonons in nanograined zinc oxide. *J. Appl. Phys.* **2010**, *108*, 053721. [CrossRef]

71. Luu, S.D.N.; Duong, T.A.; Phan, T.B. Effect of dopants and nanostructuring on the thermoelectric properties of ZnO materials. *Adv. Nat. Sci. Nanosci. Nanotechnol.* **2019**, *10*, 023001. [CrossRef]

72. Wu, X.; Lee, J.; Varshney, V.; Wohlwend, J.L.; Roy, A.K.; Luo, T. Thermal Conductivity of Wurtzite Zinc-Oxide from First-Principles Lattice Dynamics—A Comparative Study with Gallium Nitride. *Sci. Rep.* **2016**, *6*, 22504. [CrossRef] [PubMed]

73. Finn, P.A.; Asker, C.; Wan, K.; Bilotti, E.; Fenwick, O.; Nielsen, C.B. Thermoelectric Materials: Current Status and Future Challenges. *Front. Electron. Mater.* **2021**, *1*, 1–13. [CrossRef]

74. Prasad, R.; Bhame, S.D. Review on texturization effects in thermoelectric oxides. *Mater. Renew. Sustain. Energy.* **2020**, *9*, 3. [CrossRef]

75. Han, C.; Li, Z.; Dou, S. Recent progress in thermoelectric materials. *Chin. Sci. Bull.* **2014**, *59*, 2073–2091. [CrossRef]

76. Zak, A.K.; Majid, W.H.A.; Mahmoudian, M.R.; Darroudi, M.; Yousefi, R. Starch-stabilized synthesis of ZnO nanopowders at low temperature and optical properties study. *Adv. Powder Technol.* **2013**, *24*, 618–624. [CrossRef]

77. Takashiri, M.; Miyazaki, K.; Tanaka, S.; Kurosaki, J.; Nagai, D.; Tsukamoto, H. Effect of grain size on thermoelectric properties of n -type nanocrystalline bismuth-telluride based thin films. *J. Appl. Phys.* **2008**, *104*, 084302. [CrossRef]

78. Liang, X. Structure and Thermoelectric Properties of ZnO Based Materials Structure and Thermoelectric Properties of ZnO. Ph.D. Thesis, Havard University, Cambridge, MA, USA, 2013.

79. Zhang, X.; Zhao, L.-D. Thermoelectric materials: Energy conversion between heat and electricity. *J. Mater.* **2015**, *1*, 92–105. [CrossRef]

80. Guan, W.; Zhang, L.; Wang, C.; Wang, Y. Theoretical and experimental investigations of the thermoelectric properties of Al-, Bi- and Sn-doped ZnO. *Mater. Sci. Semicond. Proces.* **2017**, *66*, 247–252. [CrossRef]

81. Zhang, D.; Zhang, B.; Ye, D.; Liu, Y.; Li, S. Enhanced Al/Ni co-doping and power factor in textured ZnO thermoelectric ceramics prepared by hydrothermal synthesis and spark plasma sintering. *J. Alloys Compd.* **2016**, *656*, 784–792. [CrossRef]

82. Matiullah; Wang, C.L.; Su, W.B.; Zaman, A.; Ullah, I.; Zhai, J.Z.; Liu, D.K. Effects of sintering atmospheres on thermoelectric properties, phase, microstructure and lattice parameters c/a ratio of Al, Ga dual doped ZnO ceramics sintered at high temperature. *J. Mater. Sci. Mater. Electron.* **2018**, *29*, 9555–9563. [CrossRef]

83. Han, L.; Nong, N.V.; Hung, L.T.; Holgate, T.; Pryds, N.; Ohtaki, M.; Linderotha, S. The influence of alpha- and gamma-Al_2O_3 phases on the thermoelectric properties of Al-doped ZnO. *J. Alloys Compd.* **2013**, *555*, 291–296. [CrossRef]

84. Ohtaki, M.; Araki, K.; Yamamoto, K. High thermoelectric performance of dually doped ZnO ceramics. *J. Electron. Mater.* **2009**, *38*, 1234–1238. [CrossRef]

85. Wang, M.; Lee, K.E.; Hahn, S.H.; Kim, E.J.; Kim, S.; Chung, J.S.; Shin, E.W.; Park, C. Optical and photoluminescent properties of sol-gel Al-doped ZnO thin films. *Mater. Lett.* **2007**, *61*, 1118–1121. [CrossRef]

86. Maciá-Barber, E. *Thermoelectric Materials Advances and Applications*; Jenny Stanford Publishing: United Square, Singapore, 2015.

87. Jood, P.; Peleckis, G.; Wang, X.; Dou, S.X. Effect of gallium doping and ball milling process on the thermoelectric performance of n-type ZnO. *J. Mater. Res.* **2012**, *27*, 2278–2285. [CrossRef]

88. Lee, S.; Lee, J.; Choi, S.; Park, J. Studies of thermoelectric transport properties of atomic layer deposited gallium-doped ZnO. *Ceram. Int.* **2017**, *43*, 7784–7788. [CrossRef]